

Mohammad N. KHAN <sup>1</sup>, Dhare ALZAFIRI <sup>1</sup>

## Air bottoming combined cycle performance analyses by the combined effect of variable parameters

Received 17 October 2021, Revised 15 March 2022, Accepted 4 April 2022, Published online 23 June 2022

**Keywords:** topping cycle, air bottoming cycle, net power output, thermal efficiency, total exergy destruction, exergetic efficiency

To meet the continuous demand for energy of industrial as well as commercial sectors, researchers focus on increasing the power generating capacity of gas turbine power plants. In this regard, the combined cycle is a better solution in terms of environmental aspects and power generation as compared to a simple gas turbine power plant. The present study is the thermodynamic investigation of five possible air bottoming combined cycles in which the topping cycle is a simple gas turbine cycle, regenerative gas turbine cycle, inter-cool gas turbine cycle, reheat gas turbine cycle, and intercool-reheat gas turbine cycle. The effect of pressure ratio of the topping cycle, the turbine inlet temperature of topping cycle, and ambient temperature on net power output, thermal efficiency, total exergy destruction, and exergetic efficiency of the combined cycle have been analyzed. The ratio of the net power output of the combined cycle to that of the topping cycle is maximal in the case when the topping cycle is a simple gas turbine cycle. The ratio of net power output and the total exergy destruction of the combined cycle to those of the topping cycle decrease with pressure ratio for all the combinations under study except for the case when the topping cycle is the regenerative gas turbine cycle.

### Nomenclature

$w$	work net output, kW
$\dot{m}$	mass flow rate, kg/s
$h$	specific enthalpy, kJ/kg
$s$	specific entropy, kJ/(kg K)

✉ Dhare Alzafiri, e-mail: [dharealzafiri@gmail.com](mailto:dharealzafiri@gmail.com)

<sup>1</sup>Department of Mechanical Engineering, College of Engineering, Majmaah University, Al-Majmaah, Saudi Arabia. ORCID: M.N.K.: 0000-0002-5787-9146; D.A.: 0000-0001-8826-4075



© 2022. The Author(s). This is an open-access article distributed under the terms of the Creative Commons Attribution (CC-BY 4.0, <https://creativecommons.org/licenses/by/4.0/>), which permits use, distribution, and reproduction in any medium, provided that the author and source are cited.

---

$T$	temperature, K
$Q$	rate of heat supplied, kW
$r_p$	pressure ratio
$\varepsilon$	heat exchanger effectiveness
$LCV$	lower calorific value of fuel
$TIT$	turbine inlet temperature, K
$c_p$	specific heat capacity, kJ/kg
$\gamma$	specific heat ratio
$I_D$	exergy destruction, kW
$\eta$	efficiency
ABC	air bottoming cycle

### Subscripts

$a$	air
$g$	gasses
$f$	fuel
$t$	topping
$b$	bottoming
$c$	combined

## 1. Introduction

The generation of electrical energy most economically and efficiently from fossil fuel is one the most important topics of research nowadays. Gas turbine power plants are not efficient enough to meet the worldwide energy demand even if they utilize the latest technological developments [1–3]. The gas turbine performance deteriorates with an increase in ambient temperature and an increase in the heating rate that cause a reduction in fuel efficiency [4–6]. The appropriate technologies that have been used to improve the efficiency of the gas turbines include, among other things, the use of inlet air cooling, inter-cooling, regeneration, reheating, and steam injection gas turbines [7, 8]. There is a need to improve the performance of a gas turbine by employing various strategies such as the use of cooling techniques [9, 10]. Limited sources of fossil fuels are also one of the major factors that compel one to find an alternative source for power generation. In this regard, the combined cycle power plant plays a major role in satisfying the energy demand to a maximal extent. This option reduces fuel consumption but also reduces the environmental hazards raised by gas turbine power plants [11]. The concept of combined cycle power (CCP) plant consists in utilizing a great amount of energy of exhaust gasses from the gas turbine for running another cycle, which may be an air-bottoming or a steam bottoming one. This concept significantly impacts the power generation industry and becomes popular worldwide. The CCP plant not only helps to increase the power generating capacity of the plant but also drastically reduces the pollution caused by the exhaust gases, compared to the simple GT

cycle power plant [9, 12–14]. The CCP plant is based on the concept of generating power by utilizing the heat carried by the exhaust gases of gas turbines. Numerous investigations show that the pressure ratio [15–17], the turbine inlet temperature (*TIT*) [18–20], and the ambient temperature [21–23] are the dominating factors that increase/decrease the energy and exergy performance of CCP plants whereas the quest for efficiency improvement of the gas turbine is focused on three major areas: increasing the turbine inlet temperature, increasing turbo-machinery components efficiency, and basic cycle modifications [24–26]. Bazmi et al. [27] theoretically examine power sector development and emphasize the major section of optimization and modeling of power plants for the future demand as a tool for the ecological energy field. Chatzimouratidis et al. [28] consider the 9 end-node standards, to evaluate 10 different power plants concerning their economic, technological, and sustainability characteristics. The study emphasizes that multi-criterion analysis is required to evaluate the power plant performance. The authors concluded that for future power generation, the power plant must be operated by renewable energy. Ibrahim et al. [29] thermodynamically investigated energy and exergy analysis of gas turbine power plant components and of the overall plant. The results show that the air compressor provides maximal exergy and energy efficiency, followed by those of the gas turbine and the combustion chamber. The study also suggested some recommendations to enhance the cycle performance. Gazikhani et al. [30] investigate conventional ABC cycle performance in terms of specific fuel consumption (SFC), work output, and component exergy destruction, and compare the results with a simple gas turbine. The results show that the fuel exergy raises by 4.7–7.4% due to the components of the air bottoming cycle, and the specific work is increased by 15.4% with the decrease in SFC by 13.3%.

Several combined cycles were proposed by many researchers using different techniques to analyzed cycle. Khan et al. [31] examined the theoretically 3 different types of configurations of the combined cycle and compared them with a simple gas turbine cycle. By varying the turbine inlet temperature and pressure ratio of the topping cycle, this study evaluates three suggested combined cycle energetic performances, such as thermal efficiency, work net output, specific fuel consumption (SFC), and exergetic performance associated with exhaust gas exergy losses and exergy destruction. It was observed by the authors that the *TIT* significantly affects the energetic and exergetic performance of the suggested cycles. Ibrahim et al. [23] reviewed various types of gas turbine power plants including simple as well as complex gas turbine power plants. The study focused on major parameters that affect the plant performance and finally suggested some means for improving the gas turbine power plant performance and minimizing the losses.

Based on the above-discussed literature and other available literature, one can find that many researchers present the theoretical analysis of the air bottoming cycle in which the topping cycle is a simple gas turbine cycle [32–34]. No literature is available that provides comparative analyses of the air bottoming cycle in which the topping cycle is either a simple gas turbine cycle, a regenerative gas turbine cycle,

an intercool gas turbine cycle, a reheat gas turbine cycle, or an intercool-reheat gas turbine cycle. The present study focuses on the importance of the configuration of the gas turbine cycle as the topping cycle of the air bottoming combined cycle. The performance of the bottoming cycle depends on the temperature of exhaust gasses from the turbine of the topping cycle. It is observed that the temperature of exhaust gasses is significantly affected by the turbine inlet temperature, pressure ratio, and cycle configuration. In the case of the regenerative gas turbine cycle, the exhaust gasses temperature drastically decreases due to exchange of heat with the compressed air from the air compressor, which increases the overall thermal efficiency. However, this decrease in exhaust gasses temperature also results in a decrease in the energetic performance of the bottoming cycle. For this reason, the overall performance of the combined cycle is worsened. Therefore, this paper presents the thermodynamics analyses of the above-mentioned five sets of topping cycle of the air bottoming combined cycles. The effect of pressure ratio of the topping cycle, the turbine inlet temperature of topping cycle, and the ambient temperature on net power output, thermal efficiency, total exergy destruction, and exergetic efficiency of the combined cycle is analyzed. The results are discussed and presented graphically.

## 2. Description of air bottoming cycle

In this study, there are presented five sets of practically possible combinations of air bottoming gas turbine cycles, starting from the simple gas turbine cycle (set 1), then the regenerative gas turbine cycle (set 2), the intercool gas turbine cycle (set 3), the reheat gas turbine cycle (set 4), and the intercool-reheat gas turbine cycle (set 5). The pressure ratio of the compressor or turbine ( $r_p$ ) and turbine inlet temperature ( $TIT$ ) of the topping cycle varies from 4 to 12 and 1000 K to 1500 K, respectively. The other variable in all these cycles is the ambient temperature or air compressor inlet temperature, which varies from 25°C to 45°C. In each cycle, the air at the ambient temperature  $T_1$  enters the air compressor where it compresses to the pressure  $P_2$  and temperature  $T_2$ . In the simple gas turbine cycle and the reheat gas turbine cycle, the compressed air from the compressor directly goes to the combustion chamber, whereas in the regenerative gas turbine cycle it enters the combustion chamber via the heat exchanger. In the intercool gas turbine cycle, the compressed air from the low-pressure compressor (LPC) enters the intercooler, where its pressures remain the same but the temperature decreases, and then it enters the combustion chamber via high-pressure compressor, enters the gas turbine where it expands to low pressure and low temperature in the cases of set 1 to set 3. In the case of set 4 and set 5, the combustible product first enters the high-pressure turbine (HPT) and then the low-pressure turbine (LPT) via the reheater where it expands to low pressure and low temperature.

The combustible product from the gas turbine of the topping cycle leaves to the environment via heat exchanger where it exchanges heat with the compressed

air of the bottoming cycle. In the bottoming cycle, air at ambient temperature and ambient pressure enters the air compressor where it compresses to high pressure. The high pressure and high temperature compressed air from the air compressor enters the heat exchanger where it gains heat from the exhaust gasses of the topping cycle. This results in a further rise in the temperature of the compressed air. The compressed air from the heat exchanger enters the turbine and expands to low pressure, which produces the work output. A part of work output from the turbine is used to drive the air compressor and the remaining work is used to generate electricity by means of a generator. In this way, the bottoming cycle is completed. The general energy and exergy analysis of all cycles is given below.

### 3. Governing equations

#### 3.1. Energy and exergy analyses of topping cycle

All energy and exergy equations of the topping cycle are listed below.

Power required to run the compressor

$$(w_c) = \dot{m}_a (h_e - h_i) . \quad (1)$$

Exit temperature of air from the air compressor

$$(T)_e = (T)_i \left\{ 1 + \frac{r_p^\alpha - 1}{\eta_c} \right\} , \quad (2)$$

where  $\alpha = (\gamma - 1) / \gamma$ .

Rate of heat supplied by the combustion chamber

$$(Q) = \dot{m}_g (h_g)_e - \dot{m}_a (h_a)_i . \quad (3)$$

Power delivered by the turbine

$$(w_t) = \dot{m}_g \left[ (h_g)_i - (h_g)_e \right] . \quad (4)$$

Exit temperature of gasses from the gas turbine

$$(T)_e = (T)_i \left\{ 1 - \eta_t \left( 1 - r_p^{-\beta} \right) \right\} , \quad (5)$$

where  $\beta = (\gamma' - 1) / \gamma'$ .

Net power output

$$(w_{\text{net}})_t = w_t - w_c . \quad (6)$$

Thermal efficiency

$$(\eta_{\text{th}}) = \frac{w_{\text{net}}}{Q} . \quad (7)$$

Mass flow rate of fuel in the combustion chamber

$$\dot{m}_f = \dot{m}_a \left\{ \frac{(h_g)_e - (h_a)_i}{\eta_{\text{comb}}(LCV) - (h_g)_e} \right\}, \quad (8)$$

$$\dot{m}_g = \dot{m}_a + \dot{m}_f. \quad (9)$$

Effectiveness of the heat exchanger of the topping cycle

$$(\varepsilon)_{HE_1} = \frac{[(h_a)_e - (h_a)_i]}{(h_g)_i - (h_a)_i}. \quad (10)$$

The exit temperature of air from the heat exchanger of the topping cycle is given by

$$(T_a)_e = \left( \frac{1}{c_{pa}} \right) \left[ \varepsilon_{HE_1} (h_g)_i + (1 - \varepsilon_{HE_1}) (h_a)_i \right]. \quad (11)$$

The exergy destruction in the compressor can be written as

$$(I_D)_c = m_a T_{\text{ref}} (s_{ae} - s_{ai}). \quad (12)$$

The exergy destruction in the combustion chamber is given by

$$(I_D)_{\text{comb}} = T_{\text{ref}} \left[ \begin{aligned} & \left( m_g C_{pg} \ln \left( \frac{T_{ge}}{T_{\text{ref}}} \right) - m_g R_g \ln \left( \frac{P_{ge}}{P_{\text{ref}}} \right) \right) \\ & - \left( m_a C_{pa} \ln \left( \frac{T_{ai}}{T_{\text{ref}}} \right) - m_a R_a \ln \left( \frac{P_{ai}}{P_{\text{ref}}} \right) \right) + \Delta s_{\text{ref}} \end{aligned} \right], \quad (13)$$

where

$$T_{\text{ref}} (\Delta s_{\text{ref}}) = \Delta G_{\text{ref}} - \Delta H_{\text{ref}},$$

$$\Delta H_{\text{ref}} = \dot{m}_f (LCV)_{T_{\text{ref}}},$$

$$\text{Exergy flux}(\psi) = (\Delta G_{\text{ref}} / \Delta H_{\text{ref}}) = 1.0401 + 0.1728(h/c),$$

$$(h/c) = \text{Hydrogen to carbon ratio of fuel.}$$

The exergy destruction in turbine is given by

$$(I_D)_t = m_g T_{\text{ref}} (s_{ge} - s_{gi}). \quad (14)$$

The exergy destruction in the HRSG is given by

$$(I_D)_{\text{HRSG}} = T_{\text{ref}} \left[ m_a (s_{ae} - s_{ai}) + m_g (s_{ge} - s_{gi}) \right]. \quad (15)$$

Exergy destruction of topping cycle

$$(I_D)_t = \sum_{i=1}^n (I_D)_n. \quad (16)$$

Exergetic efficiency of topping cycle

$$(\eta_D)_t = \frac{(w_{\text{net}})_t}{(w_{\text{net}})_t + (I_D)_t}. \quad (17)$$

### 3.2. Energy and exergy analyses of bottoming cycle

All energy and exergy equations of bottoming cycle are listed below.  
Power required to run the compressor

$$(w_c)_b = \dot{m}_{ab} (h_e - h_i). \quad (18)$$

Exit temperature of air from the air compressor

$$(T)_e = (T)_i \left\{ 1 + \frac{r_{pb}^\alpha - 1}{\eta_c} \right\}, \quad (19)$$

where  $\alpha = (\gamma - 1)/\gamma$ .

Let

$$x = \eta_c \eta_t (\dot{m}_g / \dot{m}_{ab}) (c_{pg} / c_{pa}) ((T_{ab})_e)_{HE_2} / ((T_{ab})_i)_c, \quad (20)$$

$$r_{pb} = (x)^{1/(\alpha+\beta)}. \quad (21)$$

Effectiveness of the heat exchanger

$$(\varepsilon)_{HE_2} = \frac{[(h_a)_e - (h_a)_i]_b}{[(h_g)_e]_t - [(h_a)_i]_b}. \quad (22)$$

The exit temperature of air from the heat exchanger of bottoming cycle is given by

$$(T_{ab})_e = \left( \frac{1}{c_{pa}} \right) [\varepsilon_{HE_2} (h_g)_i + (1 - \varepsilon_{HE_2}) (h_{ab})_i]. \quad (23)$$

Power delivered by the turbine

$$(w_t)_b = \dot{m}_{ab} [(h_a)_i - (h_a)_e]. \quad (24)$$

Exit temperature of gasses from the gas turbine

$$(T)_e = (T)_i \left\{ 1 - \eta_t \left( 1 - r_{pb}^{-\alpha} \right) \right\}. \quad (25)$$

The net power output

$$(w_{net})_b = (w_t)_b - (w_c)_b. \quad (26)$$

The exergy destruction in the compressor can be written as

$$(I_D)_c = m_{ab} T_{ref} (s_{ae} - s_{ai}). \quad (27)$$

The exergy destruction in turbine is given by

$$(I_D)_t = m_{ab} T_{ref} (s_{ae} - s_{ai}). \quad (28)$$

The exergy destruction in the HRSG is given by

$$(I_D)_{\text{HRSG}} = T_{\text{ref}} \left[ m_{ab} (s_{ae} - s_{ai}) + m_g (s_{ge} - s_{gi}) \right]. \quad (29)$$

The exergy destruction of bottoming cycle

$$(I_D)_b = \sum_{i=1}^n (I_D)_n. \quad (30)$$

### 3.3. Energy and exergy analyses of combined cycle

All energy and exergy equations of the combined cycle are listed below.  
The net power output of the combined cycle

$$(w_{\text{net}})_{\text{comb}} = (w_{\text{net}})_t + (w_{\text{net}})_b. \quad (31)$$

Thermal efficiency of combined cycle

$$(\eta_{\text{th}})_{\text{comb}} = \frac{(w_{\text{net}})_{\text{comb}}}{Q}. \quad (32)$$

Exergy destruction of combined cycle

$$(I_D)_{\text{comb}} = \left( \sum_{i=1}^n (I_D)_n \right)_t + \left( \sum_{i=1}^n (I_D)_n \right)_b. \quad (33)$$

Exergetic efficiency of combined cycle

$$(\eta_D)_{\text{comb}} = \frac{(w_{\text{net}})_{\text{comb}}}{(w_{\text{net}})_{\text{comb}} + (I_D)_{\text{comb}}}. \quad (34)$$

The analysis of the topping cycle, bottoming cycle, and combined cycle of the present study is based on certain assumed parameters listed in Table 1.

Table 1. Key parameters of all sets under study [35–39]

Assumed parameters	
Isentropic efficiency of the turbine	0.85
Isentropic efficiency of air compressor	0.8
Efficiency of combustion chamber	1.0
The mass flow rate of air in topping and bottoming cycle	1 kg/s
The effectiveness of heat exchangers	0.9
Lower calorific value of fuel	42500 kJ/kg
Inlet pressure of air to the air compressor	1.013 bar
Specific heat of gases	1.14 kJ/(kg K)
Specific heat ratio for gases	1.4

#### 4. Results and discussion

The net power output, thermal efficiency, total exergy destruction, and exergetic efficiency of the simple gas turbine cycle (set 1), the regenerative gas turbine cycle (set 2), the intercool gas turbine cycle (set 3), the re-heat gas turbine cycle (set 4), and the intercool re-heat gas turbine cycle (set 5) are investigated parametrically by using the Engineering Equation Solver (EES) software based on the assumptions mentioned in Table 1 with the variation of pressure ratio from 4 to 12, turbine inlet temperature from 1000 K to 1500 K, and ambient temperature 25°C to 45°C.

The schematic and T-s diagram of set 1 is shown in Fig. 1. The main components of the topping and bottoming cycle are the air compressor (c), the combustion chamber (cc), the turbine (T), and the heat exchanger (H.E.). The variation of net power output and thermal efficiency of the combined cycle with respect to the pressure ratio ( $r_p$ ) of the topping cycle, turbine inlet temperature ( $TIT$ ), and ambient temperature ( $T_{ref}$ ) is shown in Fig. 2a, whereas Fig. 2b shows the variation of total exergy destruction and exergetic efficiency of the ABC cycle with respect to the pressure ratio ( $r_p$ ) of topping cycle, turbine inlet temperature ( $TIT$ ), and ambient temperature ( $T_{ref}$ ). It is observed from Fig. 2a that with an increase of ambient temperature the net power output and thermal efficiency decrease and with an increase in turbine inlet temperature the net power output and thermal efficiency increase. Similar results were reported by Khan et al. [18] and Ghazikhani et al. [30]. Also, at the particular  $T_{ref}$ , the net power output first increases and then decreases after reaching its peak value at  $r_p = 4$  when  $TIT = 1000$  K and at  $r_p = 7$  when  $TIT = 1500$  K. Similarly, at the particular  $T_{ref}$ , the thermal efficiency of the ABC cycle first increases and then decreases after reaching its peak value at  $r_p = 7$  when  $TIT = 1000$  K and at  $r_p = 12$  when  $TIT = 1500$  K. Fig. 2b shows that with an increase of ambient temperature the total exergy destruction and the exergetic efficiency of the ABC cycle decrease, whereas with an increase in turbine inlet

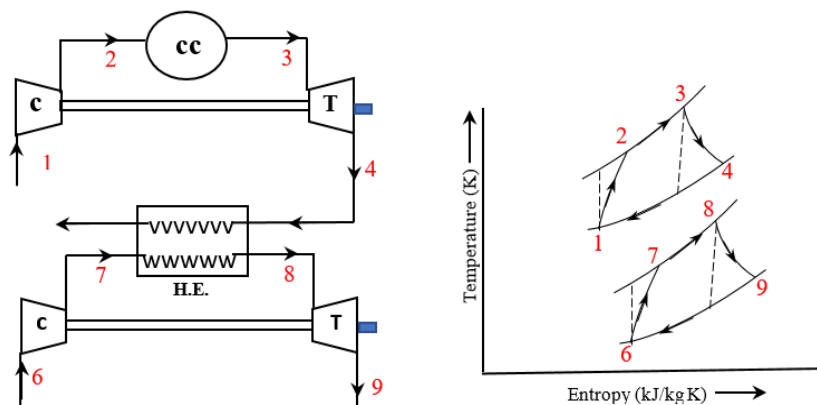


Fig. 1. Schematic and T-s diagram of set 1

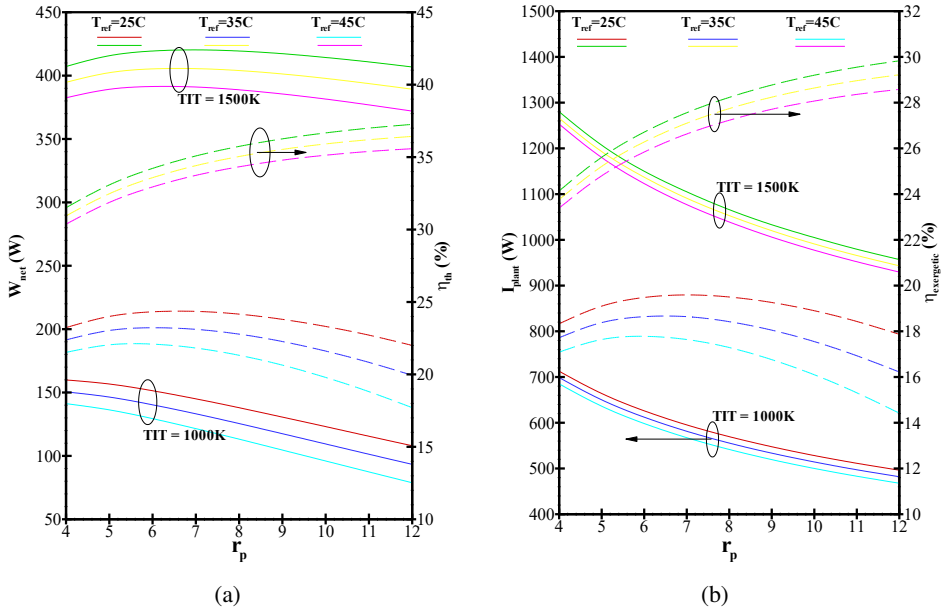


Fig. 2. Variation of  $W_{net}$ , and  $\eta_{th}$  (a) and  $I_{plant}$  and  $\eta_{exergetic}$  (b) of ABC cycle w.r.t.  $r_p$ ,  $TIT$ , and  $T_{ref}$  of set 1

temperature the total exergy destruction and the exergetic efficiency increase. Also, at the particular  $T_{ref}$ , the total exergy destruction of the ABC cycle continuously decreases with the pressure ratio and reaches minimum at  $r_p = 4$  when  $TIT = 1000$  K and  $1500$  K. Similarly, at the particular  $T_{ref}$ , the exergetic efficiency of the ABC cycle first increases and then decreases after reaching its peak value at  $r_p = 7$  when  $TIT = 1000$  K, and when  $TIT = 1500$  K, the exergetic efficiency of the ABC cycle continuously increases with the pressure ratio. The same trend was noted in the results obtained by Tiwari et al. [22]. The schematic and T-s diagram of set 2 is shown in Fig. 3. The main components of the topping cycle are the same as those of the topping cycle of set 1 with an addition of one more component that is the heat exchanger (H.E.) placed between the air compressor and the combustion chamber.

The variation of net power output and thermal efficiency of the combined cycle with respect to the pressure ratio ( $r_p$ ) of the topping cycle, turbine inlet temperature ( $TIT$ ), and ambient temperature ( $T_{ref}$ ) is shown in Fig. 4a. Fig. 4b shows the variation of total exergy destruction and exergetic efficiency of the ABC cycle with respect to the pressure ratio ( $r_p$ ) of the topping cycle, turbine inlet temperature ( $TIT$ ), and ambient temperature ( $T_{ref}$ ).

It can be seen in Fig. 4a that the net power output and thermal efficiency decrease with an increase of ambient temperature and increase with an increase in turbine inlet temperature. Also, the net power output first increases and then

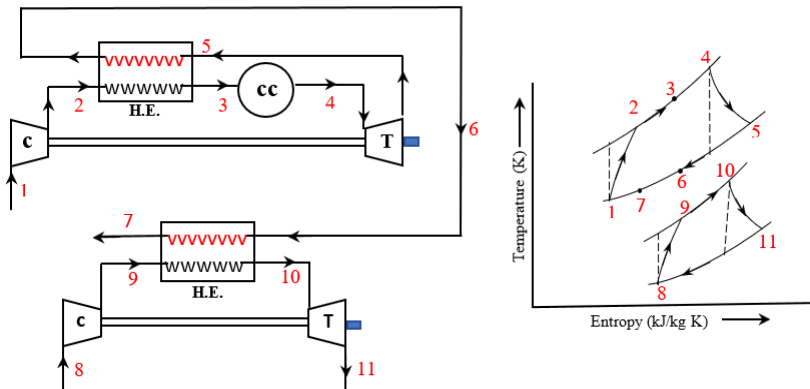


Fig. 3. Schematic and T-s diagram of set 2

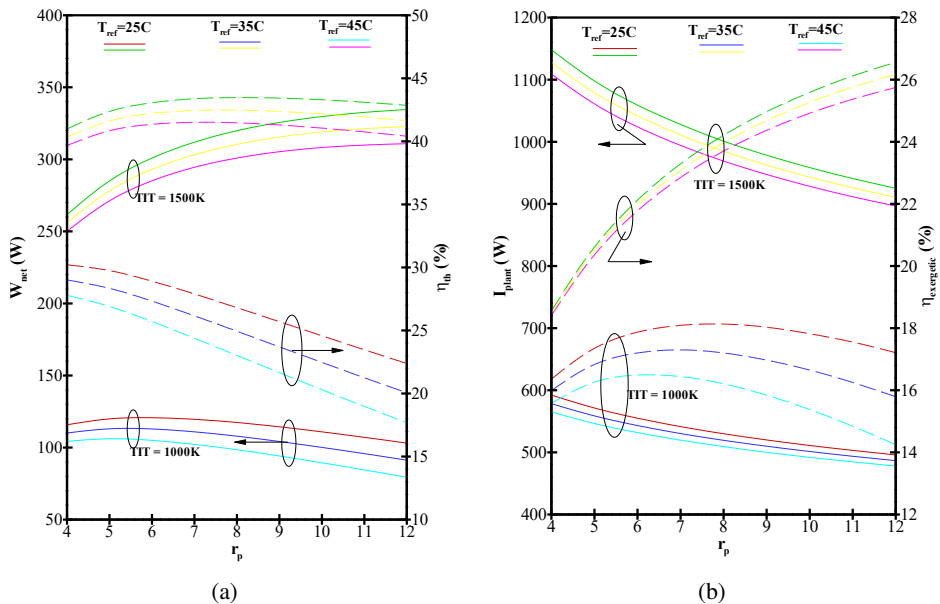


Fig. 4. Variation of  $W_{net}$ , and  $\eta_{th}$  (a) and  $I_{plant}$  and  $\eta_{exergetic}$  (b) of ABC cycle w.r.t.  $r_p$ ,  $TIT$ , and  $T_{ref}$  of set 2

decreases after reaching its peak value at  $r_p = 6$  when  $TIT = 1000$  K and at  $r_p = 12$  when  $TIT = 1500$  K. The thermal efficiency of the ABC cycle continuously decreases when  $TIT = 1000$  K, and when  $TIT = 1500$  K, the thermal efficiency first increases and then decreases slightly after reaching its peak value at  $r_p = 8$ .

Fig. 4b shows that the total exergy destruction of the ABC cycle for set 2. The total exergy destruction and the exergetic efficiency decreases with ambient temperature and increases with turbine inlet temperature. Also, at the particular  $T_{ref}$  and turbine inlet temperature, the total exergy destruction continuously decreases

whereas the exergetic efficiency increases with the pressure ratio. At  $TIT = 1000$  K, the value of pressure ratio at which the peak value of exergetic efficiency is reached increases with a decrease of ambient temperature. Almost the same trend for net power output as well as thermal efficiency was observed by Ibrahim and Rahman [40]. The schematic and T-s diagram of set 3 is shown in Fig. 5. The main components of the topping cycle are the same as in the topping cycle of set 1 with the addition of the air compressor and the intercooler, which decreases the temperature of the compressed air from the low-pressure compressor under the assumption that the pressure drop is negligible. The variation of net power output and thermal efficiency of the combined cycle with respect to the pressure ratio ( $r_p$ ) of the topping cycle, turbine inlet temperature ( $TIT$ ), and ambient temperature ( $T_{ref}$ ) is shown in Fig. 6a, whereas Fig. 6b shows the variation of total exergy destruction and exergetic efficiency of the ABC cycle with respect to the pressure ratio ( $r_p$ ) of the topping cycle, turbine inlet temperature ( $TIT$ ), and ambient temperature ( $T_{ref}$ ).

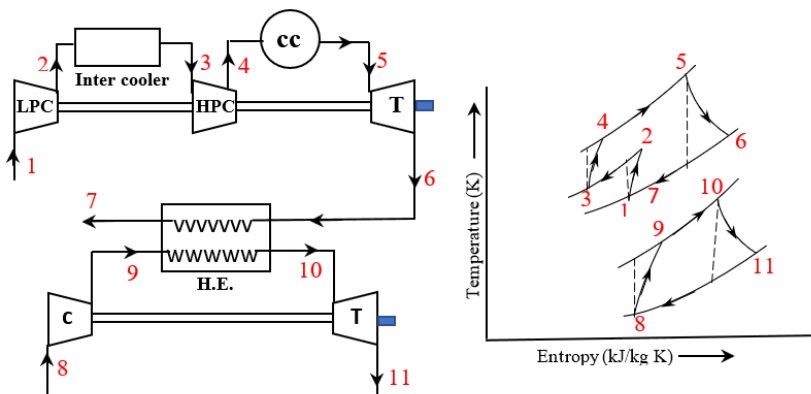


Fig. 5. Schematic and T-s diagram of set 3

It can be seen in Fig. 6a that the net power output and thermal efficiency decrease with an increase of ambient temperature and increase with an increase in turbine inlet temperature. Also, the net power output first increases and then decreases after reaching its peak value at  $r_p = 6$  when  $TIT = 1000$  K and at  $r_p = 12$  when  $TIT = 1500$  K. The thermal efficiency of the ABC cycle first increases and then decreases after reaching its peak value at  $r_p = 9$  when  $TIT = 1000$  K and at  $r_p = 12$  when  $TIT = 1500$  K. Fig. 6b shows that the total exergy destruction for set 3 decreases with an increase of ambient temperature and increases with an increase in turbine inlet temperature. Also, at a particular value of ambient temperature and turbine inlet temperature, the total exergy destruction continuously decreases whereas the exergetic efficiency continuously increases with an increase in pressure ratio. At  $TIT = 1000$  K, the effect of ambient temperature on exergetic efficiency is greater than that at  $TIT = 1500$  K. The schematic and T-s diagram of set 4 is

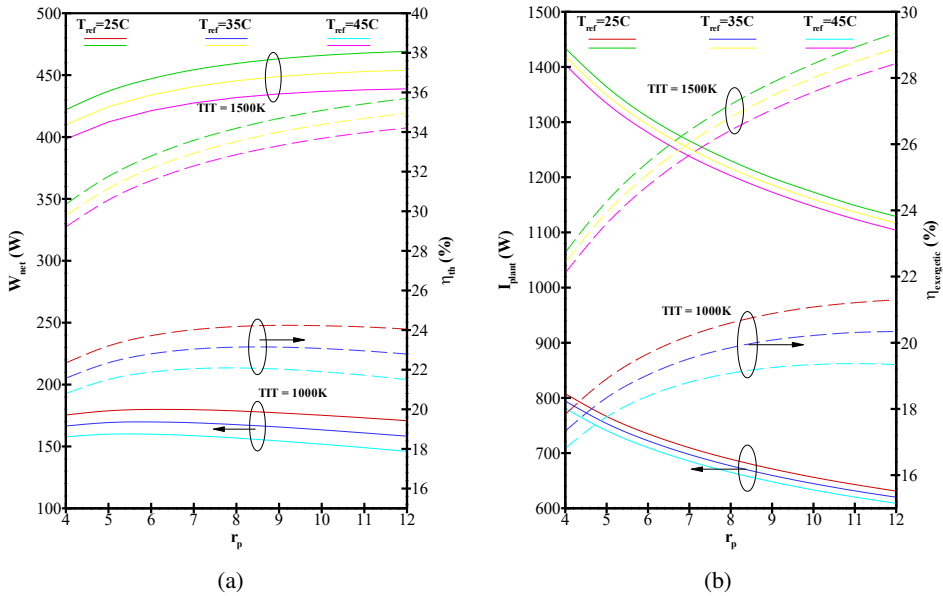


Fig. 6. Variation of  $W_{net}$ , and  $\eta_{th}$  (a) and  $I_{plant}$  and  $\eta_{exergetic}$  (b) of ABC cycle w.r.t.  $r_p$ ,  $TIT$ , and  $T_{ref}$  of set 3

shown in Fig. 7. The main components of the topping cycle are the same as in the topping cycle of set 1 with an additional gas turbine and the reheater applied for increasing the temperature of combustible gases from the high-pressure turbine with the assumption that the pressure drop is negligible. The combustible gases from the combustion chamber first expand in the high-pressure turbine then expands in the low-pressure turbine. The exhaust gasses from the low-pressure turbine leave to the environment via heat exchanger where they exchange their heat with the compressed air of the bottoming cycle.

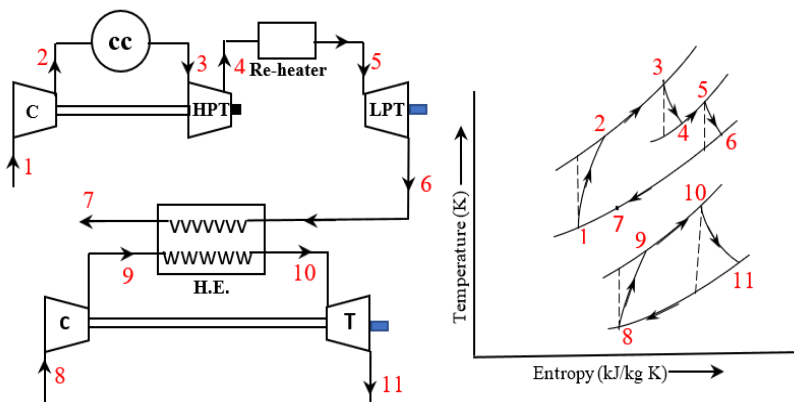


Fig. 7. Schematic and T-s diagram of set 4

The variation of net power output and thermal efficiency of the combined cycle is shown in Fig. 8a with respect to the pressure ratio ( $r_p$ ) of the topping cycle, turbine inlet temperature ( $TIT$ ), and ambient temperature ( $T_{ref}$ ), whereas Fig. 8b shows the variation of total exergy destruction and exergetic efficiency of the ABC cycle with respect to the pressure ratio ( $r_p$ ) of topping cycle, turbine inlet temperature ( $TIT$ ), and ambient temperature ( $T_{ref}$ ).

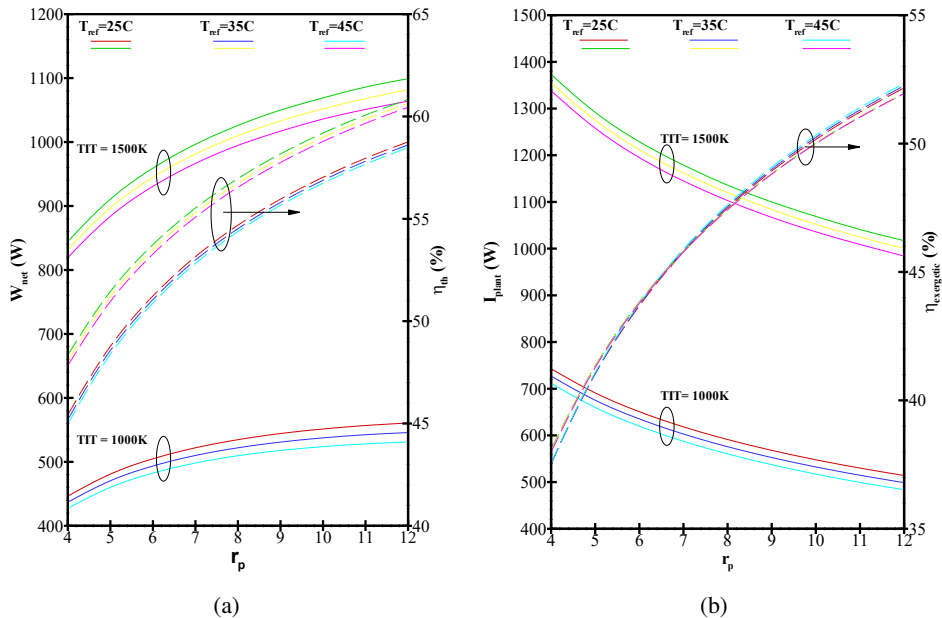


Fig. 8. Variation of  $W_{net}$ , and  $\eta_{th}$  (a) and  $I_{plant}$  and  $\eta_{exergetic}$  (b) of ABC cycle w.r.t.  $r_p$ ,  $TIT$ , and  $T_{ref}$  of set 4

As can be seen in Fig. 8a, the net power output and thermal efficiency decrease with an increase of ambient temperature and significantly increase with an increase in turbine inlet temperature. The net power output and thermal efficiency rise continuously with pressure ratio in the entire range of ambient temperature and turbine inlet temperature, but the rate of increase of the work net output grows with  $TIT$ . The thermal efficiency of the ABC cycle is least affected by the ambient temperature followed by the turbine inlet temperature. Fig. 8b shows that the total exergy destruction for set 4 decreases with an increase of ambient temperature and increases with an increase in turbine inlet temperature. The results are consistent with those obtained by Ibrahim et al. [40]. Also, at a particular ambient temperature and turbine inlet temperature, the total exergy destruction continuously decreases. The exergetic efficiency continuously increases with an increase in pressure ratio and is negligibly affected by the ambient temperature and turbine inlet temperature. The schematic and T-s diagram of set 5 is shown in Fig. 9. The main components of the topping cycle are the low-pressure compressor, the high-pressure compress-

sor, the intercooler, the combustion chamber, the high-pressure gas turbine, the reheater, and the low-pressure gas turbine. The pressure drop is negligible in the intercooler, combustion chamber, and reheater. The compressed air from the low-pressure compressor enters the intercooler where its temperature decreases to the temperature of the inlet air of the low-pressure compressor.

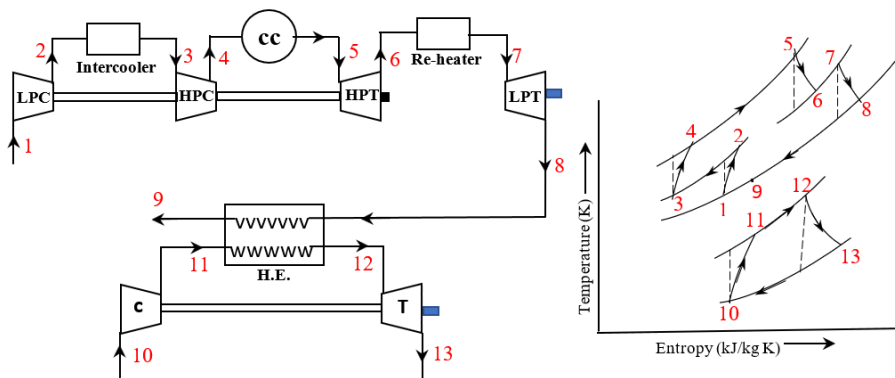


Fig. 9. Schematic and T-s diagram of set 5

This compressed air is further compressed in a high-pressure compressor before entering the combustion chamber. The combustible gases from the combustion chamber first expand in the high-pressure turbine then expands in the low-pressure turbine. The exhaust gasses from the low-pressure turbine leave to environment via heat exchanger where it exchanges its heat with the compressed air of bottoming cycle. The variation of net power output and thermal efficiency of the combined cycle is shown in Fig. 10a with respect to a pressure ratio ( $r_p$ ) of topping cycle, turbine inlet temperature ( $TIT$ ), and ambient temperature ( $T_{ref}$ ), whereas Fig. 10b shows the variation of total exergy destruction and exergetic efficiency of ABC cycle with respect to a pressure ratio ( $r_p$ ) of topping cycle, turbine inlet temperature ( $TIT$ ), and ambient temperature ( $T_{ref}$ ). It is noted from Fig. 10a that the net power output and thermal efficiency decrease with an increase of ambient temperature and significantly increase with an increase in turbine inlet temperature. Both net power output and thermal efficiency continuously with pressure ratio for the entire range of ambient temperature and turbine inlet temperature. Also, the thermal efficiency and net power output of the ABC cycle are least affected by ambient temperature. Fig. 10b shows that the total exergy destruction for set 5 and decreases with an increase of ambient temperature and increases with an increase in turbine inlet temperature. Also, at a particular value of ambient temperature and turbine inlet temperature, the total exergy destruction continuously decreases. The exergetic efficiency continuously increases with an increase in pressure ratio and is almost least affected by the ambient temperature.

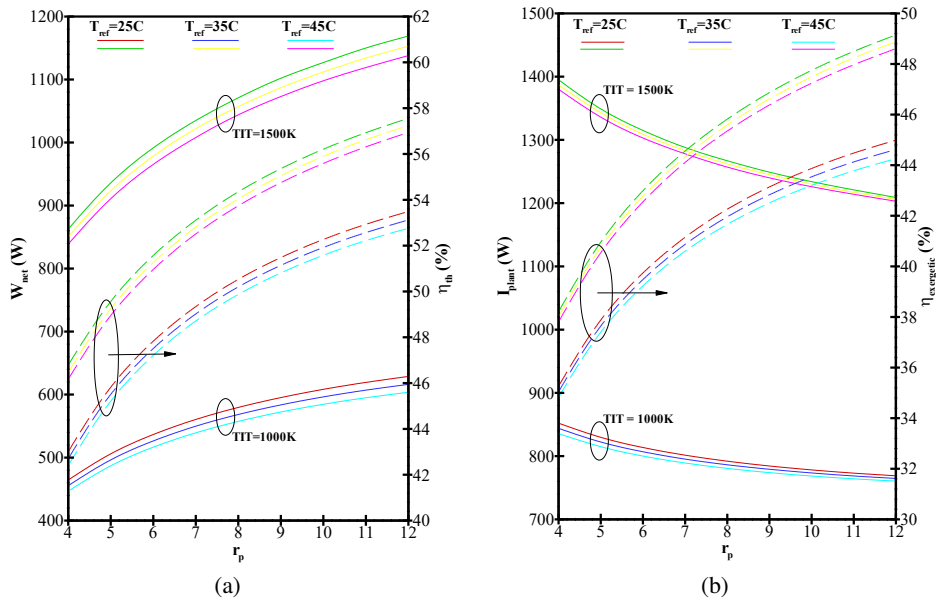


Fig. 10. Variation of  $W_{net}$ , and  $\eta_{th}$  (a) and  $I_{plant}$  and  $\eta_{exergetic}$  (b) of ABC cycle w.r.t.  $r_p$ ,  $TIT$ , and  $T_{ref}$  of set 5

The work net output, thermal efficiency, total exergy destruction, and exergetic efficiency of air bottoming combined cycle are discussed for set 1 to set 5. It is observed that work net output, thermal efficiency, total exergy destruction, and exergetic efficiency are significantly affected by the turbine inlet temperature and pressure ratio of the topping cycle. In all the above cases, the configuration of the topping cycle changes while the bottoming cycle is unchanged. The work net output for ABC of set 5 is highest followed by set 4, set 3, set 1, and then set 2 for all considering the range of pressure ratio, ambient temperature, and turbine inlet temperature. The thermal efficiency for ABC of set 3 is highest followed by set 5, set 2, set 1, and then set 3. Fig. 11 shows the variation of the ratio of work net output of the combined cycle to its topping cycle for set 1 to set 5 with respect to pressure ratio at  $TIT = 1000$  K and  $TIT = 1500$  K. It is observed that the ratio of work net output of combined cycle to its topping cycle for set 1, set 3, set 4, and set 5 decreases with pressure ratio but increases with pressure ratio in case of set 2. Fig. 11 shows the contribution of work net output of bottoming cycle in work net output of the bottoming cycle. It is noted that the contribution of the work net output of the bottoming cycle is maximal in the case of set 1, and is minimal in the case of set 2 at  $r_p = 4$ . However, at  $r_p = 12$ , contribution of the work net output of the bottoming cycle is minimal in the case of set 5. Also, the ratio of work net output of the combined cycle to its topping cycle for set 1, set 3, set 4, and set 5 increases with the turbine inlet temperature, whereas, in the case of set 2, the ratio of work net output of combined cycle to its topping cycle decreases with the turbine inlet temperature. Fig. 12 shows the variation of the ratio of the total

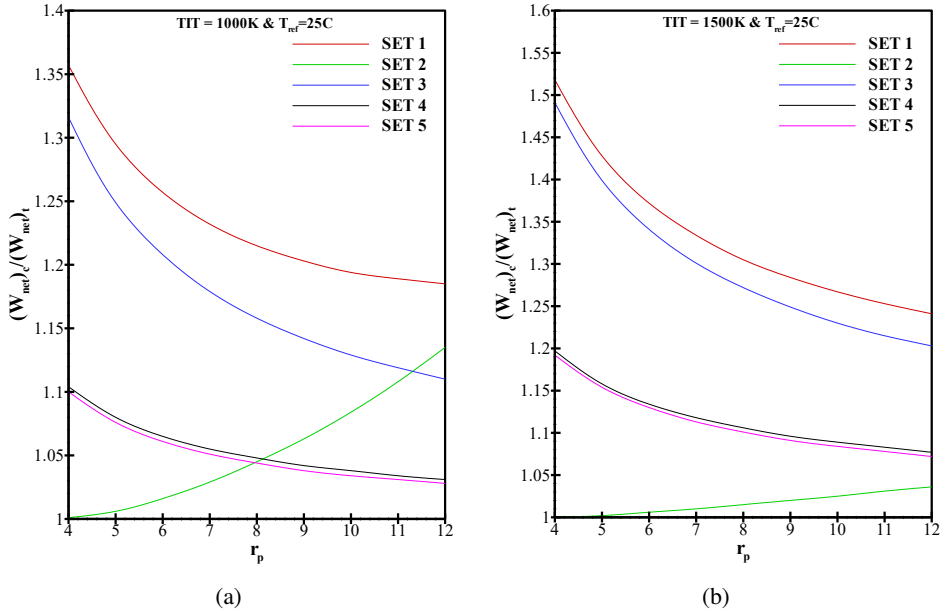


Fig. 11. Variation of the ratio of work net output of the ABC to its topping cycle at  $TIT = 1000\text{ K}$  (a), and  $TIT = 1500\text{ K}$  (b)

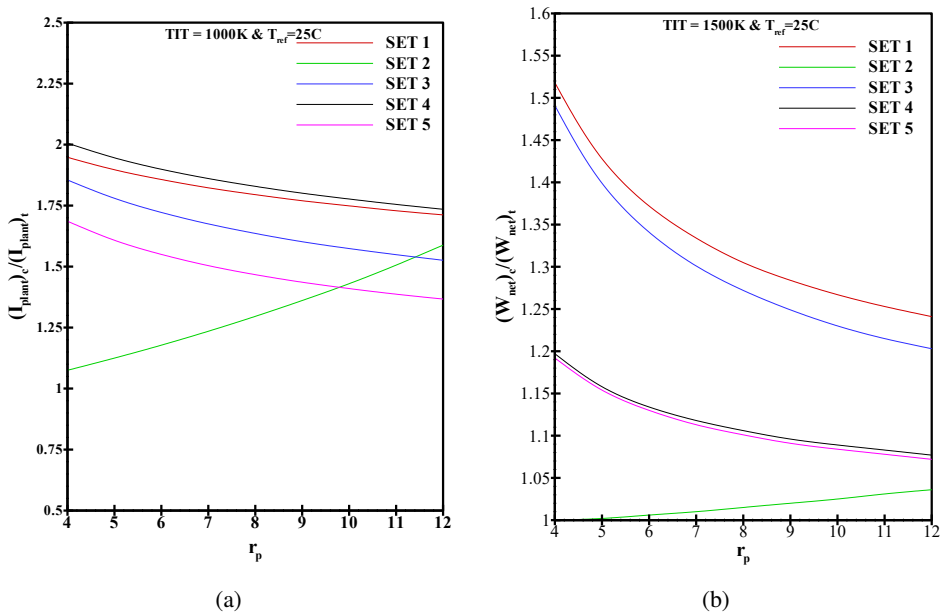


Fig. 12. Variation of the ratio of total exergy destruction of the ABC to its topping cycle at  $TIT = 1000\text{ K}$  (a), and  $TIT = 1500\text{ K}$  (b)

exergy destruction of the combined cycle to its topping cycle for the sets 1 to 5 with respect to the pressure ratio at  $TIT = 1000$  K and  $TIT = 1500$  K.

The ratio of total exergy destruction of the combined cycle to its topping cycle for set 1, set 3, set 4, and set 5 decreases with the pressure ratio but increases with the pressure ratio in the case of set 2. Also, the ratio of total exergy destruction of the combined cycle to its topping cycle for set 4 attains maximum at  $r_p = 4$  but at  $r_p = 12$ , the ratio of total exergy destruction of the combined cycle to its topping cycle for set 2 reaches maximum. The ratio of total exergy destruction of the combined cycle to its topping cycle for set 1, set 3, set 4, and set 5 increases with the turbine inlet temperature, whereas, in the case of set 2, the ratio of total exergy destruction of the combined cycle to its topping cycle decreases with the turbine inlet temperature. The maximal exergy destruction takes place in the combustion chamber, and a lesser destruction occurs in the reheater and the heat exchanger.

## 5. Conclusion

In the present study, five selected configurations of turbine cycles have been investigated parametrically for energy and exergy. Thermodynamic assessments have been effectively determined for the compressor pressure ratio from 4 to 14, ambient temperature from  $25^\circ\text{C}$  to  $45^\circ\text{C}$ , and the  $TIT$  from 1000 K to 1500 K. Based on the thermodynamic analyses, the following main conclusions have been drawn:

- It is noted that the work net output, thermal efficiency, total exergy destruction, and exergetic efficiency are significantly affected by the compressor pressure ratio and the turbine inlet temperature for all the considered configurations.
- At  $TIT = 1000$  K, the peak value of work net output exists at  $r_p = 4$  for set 1, at  $r_p = 6$  for set 2 and set 3, and at  $r_p = 12$  for set 4 and set 5 irrespective of ambient temperature. Whereas at  $TIT = 1500$  K, the peak value of work net output exists at  $r_p = 12$  for set 2, set 3, set 4, and set 5, except for set 1 where it exists at  $r_p = 7$ .
- At  $TIT = 1000$  K, the peak value of thermal efficiency exists at  $r_p = 6$  for set 1, at  $r_p = 4$  for set 2, at  $r_p = 9$  for set 3, and at  $r_p = 12$  for set 4 and set 5. Whereas at  $TIT = 1500$  K, the peak value of thermal efficiency exists at  $r_p = 12$  for set 1, set 3, set 4, and set 5 except for set 2 where it exists at  $r_p = 8$ .
- The lowest value of total exergy destruction exists at  $r_p = 12$  irrespective of  $TIT$  and ambient temperature for all the sets considered in the present study.
- The lowest value of exergetic efficiency exists at  $r_p = 4$  for the sets considered in the present study at  $TIT = 1000$  K and  $TIT = 1500$  K except for  $r_p = 12$  for the set 1 at  $TIT = 1000$  K.
- The contribution of the work net output of the bottoming cycle to the work net output of the combined cycle is maximal in the case of set 1.

From the above, it is concluded that although the net output and thermal efficiency for the combined cycle of set 5 are maximal, the work net output of the combined cycle is maximal in the case of set 1. In view of this fact, one can say that set 1 is found to be the best one in terms of cycle simplicity and its effectiveness in the bottoming cycle. The total exergy destruction of the bottoming cycle is significantly affected by the temperature of exhaust gasses from the gas turbine of the topping cycle. This is the main reason why the total exergy destruction of the bottoming cycle in the case of set 1 is maximal, whereas in the case of set 4 is greater than that of set 1 because of a lower exhaust temperature as well as the application of an additional reheater.

## References

- [1] A. Valera-Medina, A. Giles, D. Pugh, S. Morris, M. Pohl, and A. Ortwein. Investigation of combustion of emulated biogas in a gas turbine test rig. *Journal of Thermal Science*, 27:331–340, 2018. doi: [10.1007/s11630-018-1024-1](https://doi.org/10.1007/s11630-018-1024-1).
- [2] K. Tanaka and I. Ushiyama. Thermodynamic performance analysis of gas turbine power plants with intercooler: 1st report, Theory of intercooling and performance of intercooling type gas turbine. *Bulletin of JSME*, 13(64):1210–1231, 1970. doi: [10.1299/jsme1958.13.1210](https://doi.org/10.1299/jsme1958.13.1210).
- [3] H.M. Kwon, T.S. Kim, J.L. Sohn, and D.W. Kang. Performance improvement of gas turbine combined cycle power plant by dual cooling of the inlet air and turbine coolant using an absorption chiller. *Energy*, 163:1050–1061, 2018. doi: [10.1016/j.energy.2018.08.191](https://doi.org/10.1016/j.energy.2018.08.191).
- [4] A.T. Baheta and S.I.-U.-H. Gilani. The effect of ambient temperature on a gas turbine performance in part load operation. *AIP Conference Proceedings*, 1440:889–893, 2012. doi: [10.1063/1.4704300](https://doi.org/10.1063/1.4704300).
- [5] F.R. Pance Arrieta and E.E. Silva Lora. Influence of ambient temperature on combined-cycle power-plant performance. *Applied Energy*, 80(3):261–272, 2005. doi: [10.1016/j.apenergy.2004.04.007](https://doi.org/10.1016/j.apenergy.2004.04.007).
- [6] M. Ameri and P. Ahmadi. The study of ambient temperature effects on exergy losses of a heat recovery steam generator. In: Cen, K., Chi, Y., Wang, F. (eds) *Challenges of Power Engineering and Environment*. Springer, Berlin, Heidelberg, 2007. doi: [10.1007/978-3-540-76694-0\\_9](https://doi.org/10.1007/978-3-540-76694-0_9).
- [7] M.A.A. Alfellag. Parametric investigation of a modified gas turbine power plant. *Thermal Science and Engineering Progress*, 3:141–149, 2017. doi: [10.1016/j.tsep.2017.07.004](https://doi.org/10.1016/j.tsep.2017.07.004).
- [8] J.H. Horlock and W.A. Woods. Determination of the optimum performance of gas turbines. *Proceedings of the Institution of Mechanical Engineers, Part C: Journal of Mechanical Engineering Science*, 214:243–255, 2000. doi: [10.1243/0954406001522930](https://doi.org/10.1243/0954406001522930).
- [9] L. Battisti, R. Fedrizzi, and G. Cerri. Novel technology for gas turbine blade effusion cooling. In: *Proceedings of the ASME Turbo Expo 2006: Power for Land, Sea, and Air. Volume 3: Heat Transfer, Parts A and B*. pages 491–501. Barcelona, Spain. May 8–11, 2006. doi: [10.1115/GT2006-90516](https://doi.org/10.1115/GT2006-90516).
- [10] F.J. Wang and J.S. Chiou. Integration of steam injection and inlet air cooling for a gas turbine generation system. *Energy Conversion and Management*, 45(1):15–26, 2004. doi: [10.1016/S0196-8904\(03\)00125-0](https://doi.org/10.1016/S0196-8904(03)00125-0).
- [11] Z. Wang. 1.23 *Energy and air pollution*. In I. Dincer (ed.): *Comprehensive Energy Systems*, pp. 909–949. Elsevier, 2018. doi: [10.1016/B978-0-12-809597-3.00127-9](https://doi.org/10.1016/B978-0-12-809597-3.00127-9).

- [12] Z. Khorshidi, N.H. Florin, M.T. Ho, and D.E. Wiley. Techno-economic evaluation of co-firing biomass gas with natural gas in existing NGCC plants with and without CO<sub>2</sub> capture. *International Journal of Greenhouse Gas Control*, 49:343–363, 2016. doi: [10.1016/j.ijggc.2016.03.007](https://doi.org/10.1016/j.ijggc.2016.03.007).
- [13] K. Mohammadi, M. Saghaffar, and J.G. McGowan. Thermo-economic evaluation of modifications to a gas power plant with an air bottoming combined cycle. *Energy Conversion and Management*, 172:619–644, 2018. doi: [10.1016/j.enconman.2018.07.038](https://doi.org/10.1016/j.enconman.2018.07.038).
- [14] S. Mohtaram, J. Lin, W. Chen, and M.A. Nikbakht. Evaluating the effect of ammonia-water dilution pressure and its density on thermodynamic performance of combined cycles by the energy-exergy analysis approach. *Mechanika*, 23(2):18110, 2017. doi: [10.5755/j01.mech.23.2.18110](https://doi.org/10.5755/j01.mech.23.2.18110).
- [15] M. Maheshwari and O. Singh. Comparative evaluation of different combined cycle configurations having simple gas turbine, steam turbine and ammonia water turbine. *Energy*, 168:1217–1236, 2019. doi: [10.1016/j.energy.2018.12.008](https://doi.org/10.1016/j.energy.2018.12.008).
- [16] A. Khaliq and S.C. Kaushik. Second-law based thermodynamic analysis of Brayton/Rankine combined power cycle with reheat. *Applied Energy*, 78(2):179–197, 2004. doi: [10.1016/j.apenergy.2003.08.002](https://doi.org/10.1016/j.apenergy.2003.08.002).
- [17] M. Aliyu, A.B. AlQudaihi, S.A.M. Said, and M.A. Habib. Energy, exergy and parametric analysis of a combined cycle power plant. *Thermal Science and Engineering Progress*. 15:100450, 2020. doi: [10.1016/j.tsep.2019.100450](https://doi.org/10.1016/j.tsep.2019.100450).
- [18] M.N. Khan, T.A. Alkanhal, J. Majdoubi, and I. Tlili. Performance enhancement of regenerative gas turbine: air bottoming combined cycle using bypass valve and heat exchanger—energy and exergy analysis. *Journal of Thermal Analysis and Calorimetry*. 144:821–834, 2021. doi: [10.1007/s10973-020-09550-w](https://doi.org/10.1007/s10973-020-09550-w).
- [19] F. Rueda Martínez, A. Rueda Martínez, A. Toleda Velazquez, P. Quinto Diez, G. Tolentino Eslava, and J. Abugaber Francis. Evaluation of the gas turbine inlet temperature with relation to the excess air. *Energy and Power Engineering*, 3(4):517–524, 2011. doi: [10.4236/epe.2011.34063](https://doi.org/10.4236/epe.2011.34063).
- [20] A.K. Mohapatra and R. Sanjay. Exergetic evaluation of gas-turbine based combined cycle system with vapor absorption inlet cooling. *Applied Thermal Engineering*, 136:431–443, 2018. doi: [10.1016/j.applthermaleng.2018.03.023](https://doi.org/10.1016/j.applthermaleng.2018.03.023).
- [21] A.A. Alsairafi. Effects of ambient conditions on the thermodynamic performance of hybrid nuclear-combined cycle power plant. *International Journal of Energy Research*, 37(3):211–227, 2013. doi: [10.1002/er.1901](https://doi.org/10.1002/er.1901).
- [22] A.K. Tiwari, M.M. Hasan, and M. Islam. Effect of ambient temperature on the performance of a combined cycle power plant. *Transactions of the Canadian Society for Mechanical Engineering*, 37(4):1177–1188, 2013. doi: [10.1139/tcsme-2013-0099](https://doi.org/10.1139/tcsme-2013-0099).
- [23] T.K. Ibrahim, M.M. Rahman, and A.N. Abdalla. Gas turbine configuration for improving the performance of combined cycle power plant. *Procedia Engineering*, 15:4216–4223, 2011. doi: [10.1016/j.proeng.2011.08.791](https://doi.org/10.1016/j.proeng.2011.08.791).
- [24] M.N. Khan and I. Tlili. New advancement of high performance for a combined cycle power plant: Thermodynamic analysis. *Case Studies in Thermal Engineering*. 12:166–175, 2018. doi: [10.1016/j.csite.2018.04.001](https://doi.org/10.1016/j.csite.2018.04.001).
- [25] S.Y. Ebaid and Q.Z. Al-hamdan. Thermodynamic analysis of different configurations of combined cycle power plants. *Mechanical Engineering Research*. 5(2):89–113, 2015. doi: [10.5539/mer.v5n2p89](https://doi.org/10.5539/mer.v5n2p89).
- [26] R. Teflissi and A. Ataei. Effect of temperature and gas flow on the efficiency of an air bottoming cycle. *Journal of Renewable and Sustainable Energy*, 5(2):021409, 2013. doi: [10.1063/1.4798486](https://doi.org/10.1063/1.4798486).

- [27] A.A. Bazmi, G. Zahedi, and H. Hashim. Design of decentralized biopower generation and distribution system for developing countries. *Journal of Cleaner Production*, 86:209–220, 2015. doi: [10.1016/j.jclepro.2014.08.084](https://doi.org/10.1016/j.jclepro.2014.08.084).
- [28] A.I. Chatzimouratidis and P.A. Pilavachi. Decision support systems for power plants impact on the living standard. *Energy Conversion and Management*, 64:182–198, 2012. doi: [10.1016/j.enconman.2012.05.006](https://doi.org/10.1016/j.enconman.2012.05.006).
- [29] T.K. Ibrahim, F. Basrawi, O.I. Awad, A.N. Abdullah, G. Najafi, R. Mamat, and F.Y. Hagos. Thermal performance of gas turbine power plant based on exergy analysis. *Applied Thermal Engineering*, 115:977–985, 2017. doi: [10.1016/j.applthermaleng.2017.01.032](https://doi.org/10.1016/j.applthermaleng.2017.01.032).
- [30] M. Ghazikhani, I. Khazaei, and E. Abdekhodaie. Exergy analysis of gas turbine with air bottoming cycle. *Energy*, 72:599–607, 2014. doi: [10.1016/j.energy.2014.05.085](https://doi.org/10.1016/j.energy.2014.05.085).
- [31] M.N. Khan, I. Tlili, and W.A. Khan. Thermodynamic optimization of new combined gas/steam power cycles with HRSG and heat exchanger. *Arabian Journal for Science and Engineering*, 42:4547–4558, 2017. doi: [10.1007/s13369-017-2549-4](https://doi.org/10.1007/s13369-017-2549-4).
- [32] N. Abdelhafidi, İ.H. Yılmaz, and N.E.I. Bachari. An innovative dynamic model for an integrated solar combined cycle power plant under off-design conditions. *Energy Conversion and Management*, 220:113066, 2020. doi: [10.1016/j.enconman.2020.113066](https://doi.org/10.1016/j.enconman.2020.113066).
- [33] T.K. Ibrahim, M.K. Mohammed, O.I. Awad, M.M. Rahman, G. Najafi, F. Basrawi, A.N. Abd Alla, and R. Mamat. The optimum performance of the combined cycle power plant: A comprehensive review. *Renewable and Sustainable Energy Reviews*, 79:459–474, 2017. doi: [10.1016/j.rser.2017.05.060](https://doi.org/10.1016/j.rser.2017.05.060).
- [34] M.N. Khan. Energy and exergy analyses of regenerative gas turbine air-bottoming combined cycle: optimum performance. *Arabian Journal for Science and Engineering*, 45:5895–5905, 2020. doi: [10.1007/s13369-020-04600-9](https://doi.org/10.1007/s13369-020-04600-9).
- [35] A.M. Alklaibi, M.N. Khan, and W.A. Khan. Thermodynamic analysis of gas turbine with air bottoming cycle. *Energy*, 107:603–611, 2016. doi: [10.1016/j.energy.2016.04.055](https://doi.org/10.1016/j.energy.2016.04.055).
- [36] M. Ghazikhani, M. Passandideh-Fard, and M. Mousavi. Two new high-performance cycles for gas turbine with air bottoming. *Energy*, 36(1):294–304, 2011. doi: [10.1016/j.energy.2010.10.040](https://doi.org/10.1016/j.energy.2010.10.040).
- [37] M.N. Khan and I. Tlili. Innovative thermodynamic parametric investigation of gas and steam bottoming cycles with heat exchanger and heat recovery steam generator: Energy and exergy analysis. *Energy Reports*, 4:497–506, 2018. doi: [10.1016/j.egy.2018.07.007](https://doi.org/10.1016/j.egy.2018.07.007).
- [38] M.N. Khan and I. Tlili. Performance enhancement of a combined cycle using heat exchanger bypass control: A thermodynamic investigation. *Journal of Cleaner Production*, 192:443–452, 2018. doi: [10.1016/j.jclepro.2018.04.272](https://doi.org/10.1016/j.jclepro.2018.04.272).
- [39] M. Korobitsyn. Industrial applications of the air bottoming cycle. *Energy Conversion and Management*, 43(9-12):1311–1322, 2002. doi: [10.1016/S0196-8904\(02\)00017-1](https://doi.org/10.1016/S0196-8904(02)00017-1).
- [40] T.K. Ibrahim and M.M. Rahman. Optimum performance improvements of the combined cycle based on an intercooler–reheated gas turbine. *Journal of Energy Resources Technology*, 137(6):061601, 2015. doi: [10.1115/1.4030447](https://doi.org/10.1115/1.4030447).